Chapter 6
Higher Order Sliding Mode Based Accurate Tracking of Unmatched Perturbed Outputs

Leonid Fridman, Antonio Estrada, and Alejandra Ferreira de Loza

Abstract. Three approaches for higher-order sliding-mode based unmatched uncertainty compensation are summarized. Firstly, an algorithm is proposed based on the block control and quasi-continuous higher order sliding modes techniques. This method provides for the finite-time exact tracking of a smooth desired signal in spite of unmatched perturbations and allows the reduction of the controller gains in the case of partial knowledge of the system model. Thereafter, the combination of integral high-order sliding modes with the hierarchical quasi-continuous controller is proposed allowing finite-time convergence theoretically. Finally, high-order sliding mode observers are employed for exact state and uncertainties/perturbations reconstruction. A sliding mode control design is proposed which ensures theoretically exact compensation of the uncertainties/perturbations for the corresponding unmatched states based on the identified perturbation values. An inverted pendulum simulation example is considered for illustrating the feasibility of the proposed approach.

6.1 Introduction

It is a known issue that classical sliding mode (SM) control [37] is not able to compensate unmatched perturbations [11].

Leonid Fridman
Department of Control, Division of Electrical Engineering, Engineering Faculty, National Autonomous University of Mexico, UNAM, Ciudad Universitaria, 04510, Mexico, D.F.
e-mail: lfridman@unam.mx

Antonio Estrada
LUNAM Université, Ecole Centrale de Nantes, IRCCyN UMR CNRS 6597, Nantes, France
e-mail: xheper@yahoo.com

Alejandra Ferreira de Loza
University of Bordeaux, IMS-Lab, Automatic Control Group, 351 Cours de la Libération, 33405 Talence, France
e-mail: da_ferreira@yahoo.com

B. Bandyopadhyay et al. (Eds.): *Advances in Sliding Mode Control*, LNCIS 440, pp. 117–144.
DOI: 10.1007/978-3-642-36986-5_6

The combination of different robust techniques and SM has been applied to deal with systems with unmatched uncertainties [9]- [5]. In order to reduce the effects of the unmatched uncertainties [6] proposes a method that combines $\mathscr{H}_\infty$ and integral sliding mode control. The main idea is to choose such a projection matrix, ensuring that unmatched perturbations are not amplified and moreover minimized. For uncertain nonlinear systems in strict-feedback form [23], [24] developed the technique known as backstepping where a virtual control based on Lyapunov methods is constructed step by step. In a similar manner to backstepping, multiple surface sliding control is proposed in [36] to simplify the controller design of systems where model differentiation is difficult.

The combination of the backstepping design and sliding mode control is studied in [3] for systems in strict-feedback form with parameter uncertainties and it was extended to the multi-input case in [16]. The procedure proposed in [3], [16] reduces the computational load, as compared with the standard backstepping strategy, because only retains $(n-2)$ steps of the original backstepping technique, coupling them with an auxiliary second order subsystem to which a second order sliding mode control is applied. In [34] the combination of dynamical adaptive backstepping and first and second order sliding mode control is applied to both triangular and nontriangular uncertain observable minimum phase nonlinear systems.

Another approach to the problem of unmatched uncertainty compensation is based on the Nonlinear Block Controllable form (NBC-form) [31]. In [31] the conventional sliding mode technique is applied to compensate the matched perturbations. A high gain approach is used to achieve compensation of unmatched uncertainty and stabilization of the sliding mode dynamics. In [20] a sliding mode controller is designed using the combination of block control [30], a sigmoid approximation to the integral sliding mode control [38] and nested sliding mode control [1]. A coordinate transformation is applied to design a nonlinear sliding manifold. This transformation requires smoothness of each virtual control, that is why sigmoid, instead of signum functions are used. With the use of the high gain approach in [31] and sigmoid functions in [20], [1] they prove that asymptotic tracking is achieved.

In [14] a new design algorithm for systems in strict-feedback form, a special case of the BC-form, is proposed. This algorithm achieves finite-time **exact** tracking of the desired output in the presence of smooth unmatched perturbations. These features are accomplished via the use of quasi-continuous high-order sliding modes (HOSM) and a hierarchical design approach. In the first step the desired dynamic for the first state is defined by the desired tracking signal. After the first step, the desired dynamic for each state is defined by the previous one. Each virtual control is divided in two parts, the first one is intended to compensate the nominal nonlinear part of the system and the second one is aimed to achieve the desired dynamics in spite of perturbations.

Difficulties arise when initial conditions lead to big initial errors because then, the smoothness needed to achieve and keep the HOSM of each virtual control could be broken in some of them, leading to lost of control. One possible solution is to increase the gains of the HOSM term included in each virtual control, nevertheless it goes against a key motivation of the algorithm which is to reduce discontinuous

control gain via the use of information on the known nominal part of the system. The solution proposed in the present paper is to apply the integral HOSM approach reported in [25] in which the desired reference is reached by means of a previously designed auxiliary smooth trajectory that depends on the initial conditions of the error and its derivatives up to the order of the HOSM control used. Thus each state starts in the proper auxiliary sliding motion and the whole internal dynamics remains controlled since the beginning.

On the other hand, the problem of unmatched uncertainties considering only output information has been tackled in [13], [8]. In [8] a linear matrix inequalities (LMI) based method for designing an output feedback variable structure control system is presented. The author proposes an LMI based sliding surface design considering H_2 performance. Another possible solution to overcome the full state requirement is to use an observer to estimate the state. In [13] an output robust stabilization problem for a class of systems with matched and mismatched uncertainties using sliding mode techniques is considered. The idea is to use an asymptotic nonlinear observer to estimate system states, then a variable structure controller is proposed to stabilize the system. Here, a HOSM observer is employed to reconstruct the state and identify the unknown inputs theoretically exact [4]. With these informations, a sliding manifold is designed such that the system's motion along the manifold meets the specified performance: the regulation of the non-actuated states and the theoretically exact unmatched uncertainties compensation. Thus, a discontinuous control law is designed such that the system's state is driven towards the manifold and stays there for all future time, regardless of disturbances and uncertainties.

The present chapter summarizes the results of papers [14], [15], [17]. In Section 6.2.1 the class of nonlinear systems to be treated and the problem formulation are described, the Quasi-continuous control is also introduced in this section. In 6.2.2 the hierarchical design algorithm is presented. The section 6.2.3 introduces the integral HOSM approach and the modification to the hierarchical design algorithm. At the final part of the both, section 6.2.2 and 6.2.3, the corresponding proposed algorithms are applied to an example and simulation results are presented. The HOSM based exact unmatched compensation control is introduced in Section 6.2.4. The state estimation as well as the perturbations identification methodologies based on HOSM techniques are explained in In 6.2.4.1. The output sliding mode controller rejecting the unmatched uncertainty is presented in 6.2.4.2. At the end of the section, a simulation example illustrates the performance of such controller. The note then concludes with a brief comment on the proposed algorithms.

6.2 HOSM Based Unmatched Uncertainties Compensation

It is a known issue that classical sliding mode (SM) control [37] is not able to compensate unmatched perturbations [11]. Nevertheless, controllers based on HOSM algorithms may be applied in order to reject the effect of unmatched perturbations. Next, some of these schemes are presented.

6.2.1 Black Box Control via HOSM

Consider a Single-Input-Single-Output system of the form

$$\begin{array}{rcl} \dot{x}_1 & = & f_1(x_1,t)+B_1(x_1,t)x_2+\omega_1(x_1,t) \\ \dot{x}_i & = & f_i(\overline{x}_i,t)+B_i(\overline{x}_i,t)x_{i+1}+\omega_i(\overline{x}_i,t) \\ \dot{x}_n & = & f_n(x,t)+B_n(x,t)u+\omega_n(x,t) \\ i & = & 2,...,n-1 \\ \sigma & : & (t,x)\mapsto \sigma(t,x)\in \mathbb{R} \end{array} \tag{6.1}$$

where $x\in \mathbb{R}^n$ is the state vector, $x_i\in \mathbb{R}$, $\bar{x}_i=[x_1\dots x_i]^T$, and $u\in \mathbb{R}$ is the control. Moreover f_i and B_i are smooth scalar functions, ω_i is a bounded unknown perturbation term due to parameter variations and external disturbances with at least $n-i$ bounded derivatives w.r.t. system (6.1), $B_i\neq 0 \quad \forall x\in X\subset \mathbb{R}^n, t\in[0,\infty)$ and σ is the measured output. The task is to achieve $\sigma\equiv 0$.

It is assumed that system (6.1) has a constant and known relative degree r. Then it follows that $\sigma^{(r)}=h(t,x)+g(t,x)u, \quad g(t,x)\neq 0$ holds, where $h(t,x)=\sigma^{(r)}|_{u=0}$, $g(t,x)=\frac{\partial}{\partial u}\sigma^{(r)}$ if the inequalities $0<K_m\leq \frac{\partial}{\partial u}\sigma^{(r)}\leq K_M$, $|\sigma^{(r)}|_{u=0}|\leq C$ are fulfilled for some $K_m,K_M,C>0$. The trajectories of (6.1) are assumed infinitely extendible in time for any Lebesgue-measurable bounded control $u(t,x)$. The next differential inclusion is implied

$$\sigma^{(r)}\in[-C,C]+[K_m,K_M]u \tag{6.2}$$

As it was described earlier, the above problem may be solved by the Quasi-Continuous Higuer-Order Sliding Mode (QC-HOSM) controllers [26], which is constructed according to (6.3), ensuring that $\sigma=\dot{\sigma}=\ldots=\sigma^{(r-1)}=0$ is established in finite time.

$$\begin{array}{rcl} \varphi_{0,r} & = & \sigma,\ N_{0,r}=|\sigma|,\ \Psi_{0,r}=\varphi_{0,r}/N_{0,r} \\ \varphi_{i,r} & = & \sigma^{(i)}+\beta_i N_{i-1,r}^{(r-i)/(r-i+1)}\Psi_{i-1,r} \\ N_{i,r} & = & |\sigma^{(i)}|+\beta_i N_{i-1,r}^{(r-i)/(r-i+1)} \\ H_{i,r}(\cdot) & = & \varphi_{i,r}/N_{i,r}; \qquad i=0,\dots,r-1. \end{array} \tag{6.3}$$

The above result is claimed in the next theorem [26]

Theorem 6.1. *[26] Provided that $\beta_1,\dots,\beta_{r-1},\alpha>0$ are chosen sufficiently large in the listed order, the above design result in the r-sliding homogeneous controller*

$$u=-\alpha H_{r-1,r}(\sigma,\dot{\sigma},\dots,\sigma^{(r-1)}) \tag{6.4}$$

providing for the finite-time stability of (6.2),(6.4). The finite-time stable r-sliding mode $\sigma\equiv 0$ is established in system (6.1),(6.4).

In [32] compensation of unmatched perturbations is tackled using the block control approach combined with HOSM algorithms in order to consider unmodelled actuators in the controller design.

6.2.2 Model Based Application of HOSM

In [[14]], see also [[15]], a new design algorithm for systems in strict-feedback form, a special case of the BC-form, is proposed. This algorithm achieves finite-time **exact** tracking of the desired output in the presence of smooth unmatched perturbations. These features are accomplished via the use of QC-HOSM controllers and a hierarchical design approach. In the first step the desired dynamic for the first state is defined by the reference tracking signal. After the first step, the desired dynamic for each state is defined by the previous one. Each virtual control is divided into two parts, the first one is intended to compensate the nominal nonlinear part of the system and the second one is aimed at achieving the desired dynamics in spite of perturbations.

Consider the class of systems of equation (6.1), the control problem is to design a controller such that the output $y = x_1$ tracks a smooth desired reference y_d with bounded derivatives, in spite of the presence of unknown bounded perturbations. The whole state vector x is assumed to be known.

At each step i the constraint $\sigma_i = 0$ is established and kept by means of the virtual control $x_{i+1} = \phi_i$, which forms the constraint $\sigma_{i+1} = x_{i+1} - \phi_i$ for the next step.

Step 1. Defining $x_2 = \phi_1$, the next virtual controller is constructed

$$\begin{aligned} \phi_1(x_1,t,u_1) &= B_1(x_1,t)^{-1}\{-f_1(x_1,t)+u_1\} \\ u_1^{(n-1)} &= -\alpha_1 H_n(\sigma_1,\dot{\sigma}_1,\ldots,\sigma_1^{(n-1)}) \end{aligned} \tag{6.5}$$

where $\sigma_1 = x_1 - y_d$ and H_n is an n-th order sliding mode algorithm that is introduced in ϕ_1 through $n-1$ integrators. The derivatives $\sigma_1, \dot{\sigma}_1, \ldots, \sigma_1^{(n-1)}$ are calculated by means of robust differentiators with finite-time convergence [[27]].

Step i. The remaining virtual controls are constructed as follows.

$$\begin{aligned} \phi_i(\overline{x}_i,t,u_i) &= B_i(\overline{x}_i,t)^{-1}\{-f_i(\overline{x}_i,t)+u_i\} \\ u_i^{(n-i)} &= -\alpha_i H_{n-i+1}(\sigma_i,\dot{\sigma}_i,\ldots,\sigma_i^{(n-i)}) \\ \sigma_i &= x_i - \phi_{i-1}; \quad i = 2,\ldots,n. \end{aligned} \tag{6.6}$$

where H_{n-i+1} is an $n-i+1$-th order sliding algorithm. Notice that in *step n*, the real control is calculated i.e. $\phi_n = u$.

$$u = B_n(x,t)^{-1}\{-f_n(x,t)+u_n\} \tag{6.7}$$

$$u_n = -\alpha_n \operatorname{sign}(\sigma_n). \tag{6.8}$$

It is possible to smooth out the control signal by raising the order of the QC controller in each ϕ. If this is done, the super-twisting algorithm can also be used in u_n. The following theorem describes the result.

Theorem 6.2. *Provided that $\omega_i(\overline{x}_i,t)$ in system (6.1) and y_d are smooth functions with $n-i$ and n bounded derivatives respectively the above hierarchic design results in an ultimate controller u, providing for the finite time stability of $\sigma_1 = x_1 - y_d = \dot{\sigma}_1 = \ldots = \sigma_1^{(n-1)} = 0$ in system (6.1).*

Proof.
• Consider the state x_n

$$\begin{aligned} \dot{x}_n &= f_n(x,t) + B_n(x,t)u + \omega_n(x,t) \\ \text{with} \quad u &= B_n(x,t)^{-1}\{-f_n(x,t) - \alpha_n \text{sign}(\sigma_n)\}; \\ \sigma_n &= x_n - \phi_{n-1}; \quad \phi_{n-1} \text{ sufficiently smooth.} \end{aligned}$$

Thus $\dot{\sigma}_n = -\alpha_n \text{sign}(\sigma_n) + \omega_n(x,t) - \dot{\phi}_{n-1}$. Taking $\alpha_n \geq |\omega_n(x,t)| + |\dot{\phi}_{n-1}|$, provides for the appearance of a 1-sliding mode for the constraint σ_n.
• Now for the state x_{n-1}, we have

$$\begin{aligned} \dot{\sigma}_{n-1} &= \dot{x}_{n-1} - \dot{\phi}_{n-2} \\ &= f_{n-1}(\overline{x}_{n-1},t) + B_{n-1}(\overline{x}_{n-1},t)\phi_{n-1} \\ &\quad + \omega_{n-1}(\overline{x}_{n-1},t) - \dot{\phi}_{n-2} \\ &= u_{n-1} + \omega_{n-1}(\overline{x}_{n-1},t) - \dot{\phi}_{n-2} \\ \ddot{\sigma}_{n-1} &= \dot{u}_{n-1} + \dot{\omega}_{n-1}(\overline{x}_{n-1},t) - \ddot{\phi}_{n-2} \end{aligned} \tag{6.9}$$

and according to (6.6)

$$\dot{u}_{n-1} = -\alpha_{(n-1)} H_{1,2}(\sigma_{n-1}, \dot{\sigma}_{n-1}). \tag{6.10}$$

That is (6.9) takes the form:

$$\begin{aligned} \ddot{\sigma}_{n-1} &= h_{n-1}(t,x) + g_{n-1}(t,x)\dot{u}_{n-1} \\ \text{with} \quad h_{n-1}(t,x) &= \ddot{\sigma}_{n-1}|_{\dot{u}_{n-1}=0} = \dot{\omega}_{n-1} - \ddot{\phi}_{n-2} \\ g_{n-1}(t,x) &= \partial \ddot{\sigma}_{n-1} / \partial \dot{u}_{n-1}. \end{aligned} \tag{6.11}$$

If for some $K_{m_{n-1}}, K_{M_{n-1}}, C_{n-1} > 0$ the inequalities $0 < K_{m_{n-1}} \leq g_{n-1} \leq K_{M_{n-1}}$, $|h_{n-1}| \leq C_{n-1}$ are fulfilled, then the next differential inclusion is implied

$$\ddot{\sigma}_{n-1} \in [-C_{n-1}, C_{n-1}] + [K_{m_{n-1}}, K_{M_{n-1}}]\dot{u}_{n-1} \tag{6.12}$$

and controller (6.10) provides for the finite time stability of ((6.10),6.12). The finite-time stable 2-sliding mode is established for the constraint σ_{n-1}.

• It is possible to obtain an analogous equation to (6.9) for each of the remaining states, thus for the state x_1

$$\sigma_1^{(n)} = h_1(t,x) + g_1(t,x)u_1^{(n-1)} \tag{6.13}$$

$$u_1^{(n-1)} = -\alpha_1 H_{n-1,n}(\sigma_1, \dot{\sigma}_1, \ldots, \sigma_1^{(n-1)}) \tag{6.14}$$

$$\sigma_1^{(n)} \in [-C_1, C_1] + [K_{m_1}, K_{M_1}]u_1^{(n-1)} \tag{6.15}$$

the differential inclusion (6.15) is implied for some constants K_{m_1}, K_{M_1} and C_1. The controller (6.14) provides for the finite time stability of (6.15). The finite time stable n-sliding mode is established for the constraint σ_1. □

Due to the dependence on states of functions in (6.13), the inclusion (6.15) may be ensured only locally. The same applies to the inclusion obtained for each virtual control.

6.2.2.1 Example

Consider the perturbed third order system

$$\begin{aligned} \dot{x}_1 &= 2\sin(x_1) + 1.5x_2 + \omega_1(x_1,t) \\ \dot{x}_2 &= 0.8x_1x_2 + x_3 + \omega_2(\overline{x}_2,t) \\ \dot{x}_3 &= -x_3^2 + 2u + \omega_3(x,t) \end{aligned} \tag{6.16}$$

functions ω_1, ω_2 are unmatched bounded perturbations and function ω_3 is a matched bounded perturbation; these functions were defined as follows

$$\begin{aligned} \omega_1(x_1,t) &= 0.2\sin(t) + 0.1x_1 + 0.12 \\ \omega_2(\overline{x}_2,t) &= 0.3\sin(2t) + 0.2x_1 + 0.2x_2 - 0.4 \\ \omega_3(x,t) &= 0.2\sin(2t) + 0.2x_1 + 0.3x_2 + 0.2x_3 + 0.3. \end{aligned}$$

Tracking of $y_d = 2\sin(0.15t) + 4\cos(0.1t) - 4$ by x_1 is desired.

• Step 1. According to the tracking objective, the first error signal is defined as $\sigma_1 = x_1 - y_d$ and the first virtual controller as follows

$$\begin{aligned} \phi_1 &= \frac{1}{1.5}\{-2\sin(x_1) + u_1\}; \\ \ddot{u}_1 &= -\alpha_1 H_{2,3}(\sigma_1, \dot{\sigma}_1, \ddot{\sigma}_1) \\ H_{2,3} &= \frac{\ddot{\sigma}_1 + 2(|\dot{\sigma}_1| + |\sigma_1|^{2/3})^{-1/2}(\dot{\sigma}_1 + |\sigma_1|^{2/3}\mathrm{sign}(\sigma_1))}{|\ddot{\sigma}_1| + 2(|\dot{\sigma}_1| + |\sigma_1|^{2/3})^{1/2}} \end{aligned}$$

• Step 2. Defining $\sigma_2 = x_2 - \phi_1$, the next expression corresponds to ϕ_2

$$\begin{aligned} \phi_2 &= -0.8x_1x_2 + u_2 \\ \dot{u}_2 &= -\alpha_2 H_{1,2}(\sigma_2, \dot{\sigma}_2) \\ H_{1,2} &= \frac{\dot{\sigma}_2 + |\sigma_2|^{1/2}\mathrm{sign}(\sigma_2)}{|\dot{\sigma}_2| + |\sigma_2|^{1/2}} \end{aligned}$$

• Step 3. With $\sigma_3 = x_3 - \phi_2$, the real control is

$$u = \frac{1}{2}\{x_3^2 + u_3\}$$
$$u_3 = -\alpha_3 \text{sign}(\sigma_3).$$

Results obtained in simulation are shown in figures (6.1)-(6.5), using $\alpha_1 = 6$, $\alpha_2 = 10, \alpha_3 = 16$ and the initial conditions $x_\circ = [0.1,\ 0,\ 0]^T$.

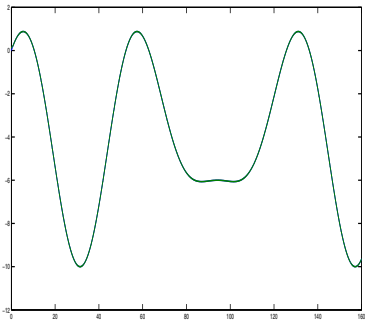

Fig. 6.1 Signals x_1 and y_d

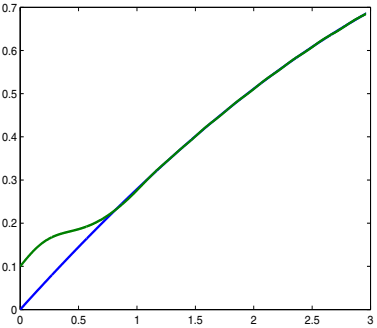

Fig. 6.2 Zoom in of the x_1 and y_d signals

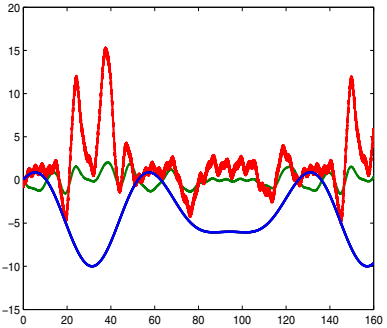

Fig. 6.3 States x_1, x_2 and x_3

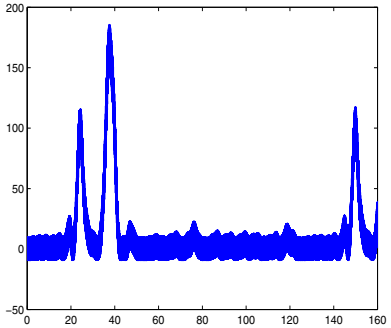

Fig. 6.4 Control signal

Since $\sigma_1 = x_1 - y_d$, straightforward algebra reveals that $u_1 = \dot{y}_d - \omega_1$ has to be accomplished in order to achieve that x_1 tracks y_d. Figure (6.5) depicts the fulfilling of the aforementioned equality.

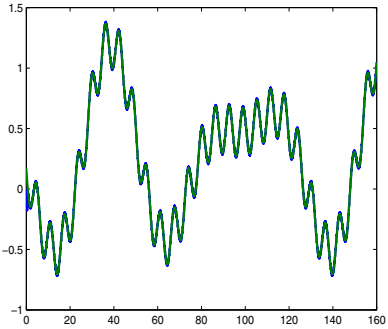

Fig. 6.5 Signals u_1 and $\dot{y}_d - \omega_1$

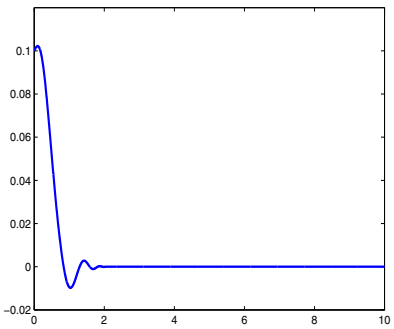

Fig. 6.6 Error signal σ_1

6.2.2.2 Example: Smoothness of the Control Signal

Consider the same nonlinear system (6.16) of the previous example. We apply the same control design procedure, but now, increasing by one the order of the QC-HOSM control present, on each virtual controller, with the aim of obtaining a smooth real control signal u.

• Step 2. The tracking error signal is $\sigma_1 = x_1 - y_d$ and next is the expression for the first virtual control

$$\phi_1(t, x_1, \sigma_1) = \frac{1}{1.5}\{-2\sin(x_1) + u_1\}$$
$$u_1^{(3)} = -\alpha_1 H_{3,4}(\sigma_1, \dot{\sigma}_1, \ddot{\sigma}_1, \dddot{\sigma}_1)$$

where

$$H_{3,4} = \Big\{ \dddot{\sigma}_1 + 3[\ddot{\sigma}_1 + (|\dot{\sigma}_1| + 0.5|\sigma_1|^{3/4})^{-1/3}(\dot{\sigma}_1 + 0.5|\sigma|^{3/4}\text{sign}(\sigma_1))] \times [|\ddot{\sigma}_1| + (|\dot{\sigma}_1| + 0.5|\sigma_1|^{3/4})^{2/3}]^{1/2} \Big\} / \Big\{ |\dddot{\sigma}_1| + 3[|\ddot{\sigma}_1| + (|\dot{\sigma}_1| + 0.5|\sigma_1|^{3/4})^{2/3}]^{1/2} \Big\}$$

• Step 2. The new error signal $\sigma_2 = x_2 - \phi_1$, is used for the next virtual control

$$\phi_2 = -0.8x_1x_2 + u_2$$
$$\ddot{u}_2 = -\alpha_2 H_{2,3}(\sigma_2, \dot{\sigma}_2, \ddot{\sigma}_2)$$

where

$$H_{2,3} = \frac{\ddot{\sigma}_2 + 2(|\dot{\sigma}_2| + |\sigma_2|^{2/3})^{-1/2}(\dot{\sigma}_2 + |\sigma_1|^{2/3}\text{sign}(\sigma_2))}{|\ddot{\sigma}_2| + 2(|\dot{\sigma}_2| + |\sigma_2|^{2/3})^{1/2}}$$

• Step 3. For the real control, defining $\sigma_3 = x_3 - \phi_2$, one has

$$u = -0.8x_1x_2 + u_3$$
$$\dot{u}_3 = -\alpha_3 H_{1,2}(\sigma_3, \dot{\sigma}_3)$$
$$H_{1,2}(\sigma_3, \dot{\sigma}_3) = \frac{\dot{\sigma}_3 + |\sigma_3|^{1/2}\text{sign}(\sigma_3)}{|\dot{\sigma}_3| + |\sigma_3|^{1/2}}$$

That is, the term u_3 in u, is a 2nd order QC-HOM introduced through one integrator. In Figures (6.7) and (6.8) the new control u and the corresponding new error signal σ_1 are plotted. The Figures (6.9) and (6.10) are zoomed views of the previously obtained non smooth control signal and the new smooth control.

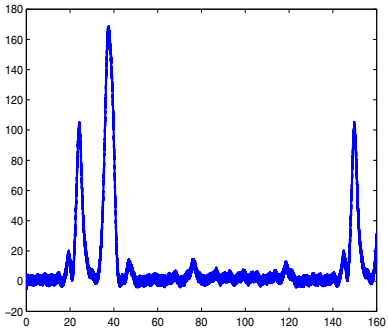

Fig. 6.7 Smooth control signal u

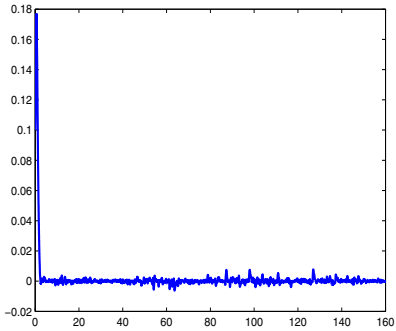

Fig. 6.8 Error signal σ_1

6.2.3 Hierachical Design Using Integral HOSM Approach

In order to illustrate the convenience of the integral HOSM approach in combination with the design algorithm presented in previous section, consider the state x_n of system (6.1) and recall the first step of the convergence proof for the control (6.7):

• For the state n

$$\dot{x}_n = f_n + B_n u + \omega_n(x,t)$$
$$\text{with} \quad u = B_n^{-1}\{-f_n + \alpha_n \text{sign}(\sigma_n)\}$$
$$\sigma_n = x_n - \phi_{n-1}; \quad \phi_{n-1} \text{ sufficiently smooth.}$$

Then $\dot{\sigma}_n = -\alpha_n \text{sign}(\sigma_n) + \omega_n(x,t) + \dot{\phi}_{n-1}$ and taking $\alpha_n \geq |\omega_n| + |\dot{\phi}_{n-1}|$ provides for the appearance of a 1-sliding mode for the constraint σ_n after a finite time T_n. Thus the subsystem

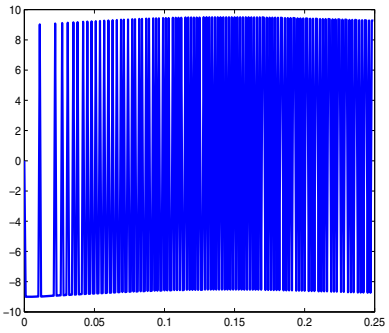

Fig. 6.9 Zoom in of non smooth control u

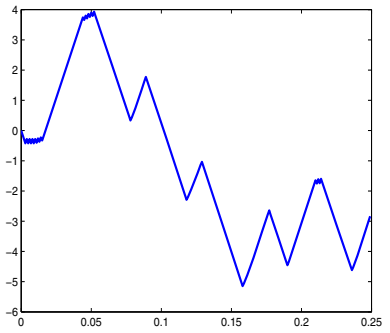

Fig. 6.10 Zoom in of smooth control u

$$\dot{x}_{n-1} = f_{n-1} + B_{n-1}x_{n-1} + \omega_{n-1}(\overline{x}_{n-1}, t)$$

could be unstable in the transient, when $x_n \neq \phi_{n-1}$. The same can be said, unless the system is bounded-input-bounded-state (BIBS), for each of the remaining states used as virtual controls before they reach the desired dynamics.

In order to overcome the problem of transient dynamics, the application of the integral HOSM approach reported in [[25]] is proposed. The main idea is that each virtual control starts in the sliding mode of the proper order from the very beginning. The procedure is as follows:

Consider the r-sliding controller (6.3) and suppose a transient trajectory $\sigma(t,x(t)) = \rho(t)$, $t_0 \leq t \leq t_f$ such that:

$$\left.\begin{array}{c} \rho(t_0) = \sigma(t_0), \ldots, \rho^{(j)}(t_0) = \sigma^{(j)}(t_0) \\ j = 1, \ldots, r-1; \quad \rho(t) \equiv 0 \; \forall t \geq t_f \end{array}\right\} \tag{6.17}$$

Integral r-sliding mode. Let $\rho^{(r-1)}(t)$ be a Lipschitz function, then it has a globally bounded derivative $\rho^{(r)}(t)$ almost everywhere, and the new output $\Sigma(t,x) = \sigma(t,x) - \rho(t)$ satisfies

$$0 < K_m \leq \frac{\partial}{\partial u}\Sigma^{(r)} \leq K_M, |\Sigma^{(r)}|_{u=0}| \leq C$$

with some changed constants $K_m, K_M, C > 0$.
Let the $(r-1)-$smooth function $\rho(t)$ satisfying (6.17) have the form

$$\rho = (t - t_f)^r (c_0 + c_1(t - t_0) + \ldots + c_{r-1}(t - t_0)^{r-1}). \tag{6.18}$$

Parameters c_i are now to be found from conditions (6.17) after t_f is assigned. In order to avoid the necessity of very large control values to reach the $r-$sliding mode

$\overrightarrow{\sigma}(t_0) = 0$ (i.e., $\sigma = \dot{\sigma} = \ldots = \sigma^{(r-1)} = 0$) due to far distanced initial values, or a very low convergence rate if $\overrightarrow{\sigma}(t_0)$ is close to zero instead of a constant, let $t_f - t_0$ be a continuous positive-definite r-sliding homogeneous function of the initial conditions, $\overrightarrow{\sigma}(t_0)$, and of homogeneity degree 1, i.e.,

$$t_f - t_0 = T(\overrightarrow{\sigma}(t_0)), \quad T(d_\kappa \overrightarrow{\sigma}) = \kappa T(\overrightarrow{\sigma}) \; \forall \kappa > 0. \tag{6.19}$$

Theorem 6.3. *[[25]] The function $\rho(t - t_0, \overrightarrow{\sigma}(t_0))$ is uniquely determined by (6.17), (6.18), (6.19). Then with any sufficiently large α, independent of the initial conditions $\overrightarrow{\sigma}(t_0)$, the controller (6.20):*

$$u = \alpha H_{r-1,r}(\Sigma, \dot{\Sigma}, \ldots, \Sigma^{(r-1)}) \tag{6.20}$$
$$\Sigma(t,x) = \begin{cases} \sigma(t,x) - \rho(t - t_0, \overrightarrow{\sigma}(t_0)), & t_0 \le t \le t_0 + T(\overrightarrow{\sigma}(t_0)) \\ \sigma(t,x), & t \ge t_0 + T(\overrightarrow{\sigma}(t_0)) \end{cases}$$

establishes the finite-time-stable r-sliding mode $\sigma \equiv 0$ with the transient time (6.19). The equality $\sigma(t, x(t)) = \rho(t - t_0, \overrightarrow{\sigma}(t_0)))$ is kept during the transient process.

The function used in this paper for $T(\overrightarrow{\sigma}(t_0))$ is the one reported in [[25]], whose expression is

$$T(\overrightarrow{\sigma}(t_0)) = \lambda(|\sigma(t_0)|^{p/r} + |\dot{\sigma}(t_0)|^{p/(r-1)} + |\sigma^{(r-1)}(t_0)|^p)^{1/p}; \quad p, \lambda > 0. \tag{6.21}$$

As previously mentioned the stability advantages of integral HOSM, obtained through the use of the knowledge of the initial conditions of the system will be used in the hierarchical design; the details are explained next.

6.2.3.1 Modification of the Hierarchical QC-HOSM Controller

The modification consists in the substitution of each restriction σ_i for a new one, $\Sigma_i = \sigma_i - \rho_i$, as follows.

Step i. The i-th sliding surface is chosen as $\Sigma_i = \sigma_i - \rho_i$ where $\sigma_i = x_i - \phi_{i-1}$ (with the exception $\sigma_1 = x_1 - y_d$).

$$\begin{aligned} \phi_i(\bar{x}_i, t, u_i) &= B_i(\bar{x}_i, t)^{-1}\{-f_i(\bar{x}_i, t) + u_i\} \\ u_i^{(n-i)} &= -\alpha_i H_{n-i,n-i+1}(\Sigma_i, \dot{\Sigma}_i, \ldots, \Sigma_i^{(n-i)}). \end{aligned} \tag{6.22}$$

$H_{n-i,n-i+1}$ is defined as in (6.3), obviously using $\sigma = \Sigma_i$ in those equations and where ρ_i fulfills condition (6.17):

$$\left.\begin{aligned} \rho_i(t_0) = \sigma(t_0), \ldots, \rho_i^{(n-i)}(t_0) = \sigma_i^{(n-i)}(t_0) \\ \rho_i(t) \equiv 0 \; \forall t \ge t_{fi} \end{aligned}\right\} \tag{6.23}$$

and is constructed according to (6.18) setting $r = n - i + 1$. The equation for (6.19), depending on the index i, is

$$T(\overrightarrow{\sigma_i}(t_0)) = \lambda_i(|\sigma_i(t_0)|^{p/n-i+1} + |\dot{\sigma}_i(t_0)|^{p/(n-i)} + \ldots + |\sigma_i^{(n-i)}(t_0)|^p)^{1/p}. \quad (6.24)$$

Step n. $\Sigma_n = \sigma_n - \rho_n$ where $\sigma_n = x_n - \phi_{n-1}$.

$$u = B_n(x,t)^{-1}\{-f_n(x,t) + u_n\} \quad (6.25)$$
$$\text{where } u_n = -\alpha_n sign(\Sigma_n).$$

Theorem 6.4. *If system (6.1) is BIBS then provided that ω_i and y_d are smooth functions with $n-i$ and n bounded derivatives respectively the above hierarchic design results in the controller (6.25) that assures the finite time stability of $\sigma_1 = x_1 - y_d = \dot{\sigma}_1 = \ldots = \sigma_1^{(n-1)} = 0$ in system (6.1) independently of their initial conditions $x(t_0)$.*

Remark 6.1. Observe that the BIBS condition is only a sufficient but not necessary condition as it can be seen in the convergence proof.

Proof.
• Consider the state x_n

$$\dot{x}_n = f_n + B_n u + \omega_n(x,t)$$
$$\text{with} \quad u = B_n^{-1}\{-f_n + \alpha_n sign(\Sigma_n)\}$$
$$\Sigma_n = \sigma_n - \rho_n,\ \sigma_n = x_n - \phi_{n-1},\ \phi_{n-1} \text{ sufficiently smooth.}$$

Then $\dot{\Sigma}_n = -\alpha_n sign(\sigma_n) + \omega_n(x,t) + \dot{\phi}_{n-1} - \dot{\rho}_n$ and taking $\alpha_n \geq |\omega_n| + |\dot{\phi}_{n-1}| + |\dot{\rho}_n|$ provides for the appearance of a 1-sliding mode for the constraint Σ_n after $t = t_0$, i.e. since the beginning, and for σ_n after $T_n = t_{fn} - t_0 = \lambda_n(|\sigma_n(t_0)|)$ choosing $p = 1$ for equation (6.24).

• Now for the state x_{n-1}, with ϕ_{n-1} defined according to (6.22) and $\Sigma_{n-1} = \sigma_{n-1} - \rho_{n-1}$, $\sigma_{n-1} = x_{n-1} - \phi_{n-2}$ then:

$$\begin{aligned}\dot{\Sigma}_{n-1} &= \dot{x}_{n-1} - \dot{\phi}_{n-2} - \dot{\rho}_{n-1} \\ &= f_{n-1} + B_{n-1}x_n + \omega_{n-1} - \dot{\rho}_{n-1} - \dot{\phi}_{n-2} \\ &= f_{n-1} + B_{n-1}(\phi_{n-1} + \rho_{n-1}) + \omega_{n-1} - \dot{\rho}_{n-1} - \dot{\phi}_{n-2}.\end{aligned}$$

The function f_{n-1}, may not be compensated right from $t = t_0$ because of the arbitrary initial condition of x_n. However due to the BIBS condition x_{n-1} remains bounded and after $t = t_0 + T_n$, when $x_n = \phi_{n-1}$:

$$\begin{aligned}\dot{\Sigma}_{n-1} &= u_{n-1} + \omega_{n-1}(\overline{x}_{n-1}, t) - \dot{\rho}_n - \dot{\phi}_{n-2} \\ \ddot{\Sigma}_{n-1} &= \dot{u}_{n-1} + \dot{\omega}_{n-1}(\overline{x}_{n-1}, t) - \ddot{\rho}_n - \ddot{\phi}_{n-2}\end{aligned} \quad (6.26)$$

that is (6.26) takes the form

$$\ddot{\Sigma}_{n-1} = h_{n-1}(t,x) + g_{n-1}(t,x)\dot{u}_{n-1} \tag{6.27}$$

$$\text{with} \quad h_{n-1}(t,x) = \ddot{\Sigma}_{n-1}|_{u_{n-1}=0};\ g_{n-1}(t,x) = \frac{\partial}{\partial \dot{u}_{n-1}}\ddot{\Sigma}_{n-1}$$

$$\dot{u}_{n-1} = -\alpha_{n-1}H_{1,2}(\Sigma_{n-1}, \dot{\Sigma}_{n-1}). \tag{6.28}$$

If for some $K_{m_{n-1}}, K_{M_{n-1}}, C_{n-1} > 0$ the inequalities $0 < K_{m_{n-1}} \leq \frac{\partial}{\partial \dot{u}_{n-1}}\ddot{\Sigma}_{n-1} \leq K_{M_{n-1}}$ and $|\ddot{\Sigma}_{n-1}|_{\dot{u}_{n-1}=0}| \leq C_{n-1}$ holds, the next differential inclusion is implied

$$\ddot{\Sigma}_{n-1} \in [-C_{n-1}, C_{n-1}] + [K_{m_{n-1}}, K_{M_{n-1}}]\dot{u}_{n-1} \tag{6.29}$$

and controller (6.28) keeps (since it was established from t_0) stability of (6.29), (6.28). The finite-time stable 2-sliding mode is maintained for the constraint Σ_{n-1} from t_0 and for σ_{n-1} after $t_{fn-1} = t_0 + T_n$.

The same procedure can be applied to each one of the states of (6.1). □

Remark 6.2. As it was previously mentioned it becomes clear that the BIBS condition is not a necessary one, it will suffice that in each subsystem of (6.1)

$$\dot{x}_i = f_i(\bar{x}_i, t) + B_i(\bar{x}_i, t)x_{i+1} + \omega_i(\bar{x}_i, t)$$

x_i remains bounded with the input x_{i+1} bounded, at least during the time interval $t < t_{fi}$; because after that time f_i is compensated.

Notice that, with the use of integral HOSM in each virtual control, it is possible to introduce suitable dynamics on each of them. If direct application is used, in which only the input and the output is considered, this is not possible.

6.2.3.2 Example

Consider the perturbed nonlinear system (6.16), rewritten here along with the control problem statement for the reader convenience

$$\begin{aligned} \dot{x}_1 &= 2\sin(x_1) + 1.5x_2 + \omega_1(x_1, t) \\ \dot{x}_2 &= 0.8x_1x_2 + x_3 + \omega_2(\bar{x}_2, t) \\ \dot{x}_3 &= -1.5x_3^2 + 2u + \omega_3(x, t) \end{aligned} \tag{6.30}$$

where functions ω_1, ω_2 are the unmatched bounded perturbations and function ω_3 is the matched perturbation. These functions were defined as follows

$$\begin{aligned}\omega_1(x_1,t) &= 0.2\sin(t)+0.1x_1+0.12\\ \omega_2(\bar{x}_2,t) &= 0.3\sin(2t)+0.2x_1+0.2x_2-0.4\\ \omega_3(x,t) &= 0.2\sin(2t)+0.2x_1+0.3x_2+0.2x_3+0.3\end{aligned}$$

a controller that achieves tracking of $y_d = 2\sin(0.15t)+4\cos(0.1t)-4$ by x_1 is desired. In addition to the previous perturbations the nominal compensation term of the first two virtual controls is not exact.

The first sliding surface is $\Sigma_1 = \sigma_1 - \rho_1,\ \sigma_1 = x_1 - y_d$, and the virtual control for x_1:

$$\begin{aligned}\phi_1(x_1,t,u_1) &= \frac{1}{1.5}\{-1.8\sin(x_1)+u_1\}\\ \dot{u}_1^{(2)} &= -\alpha_1 H_{2,3}(\Sigma_1,\dot{\Sigma}_1,\ddot{\Sigma}_1);\end{aligned}$$

$$H_{2,3}(\Sigma_1,\dot{\Sigma}_1,\ddot{\Sigma}_1) = \frac{\ddot{\Sigma}_1 + 2(|\dot{\Sigma}_1|+|\Sigma_1|^{2/3})^{-1/2}(\dot{\Sigma}_1+|\Sigma_1|^{2/3}\mathrm{sign}(\Sigma_1))}{|\ddot{\Sigma}_1|+2(|\dot{\Sigma}_1|+|\Sigma_1|^{2/3})^{1/2}}$$

$$\begin{aligned}\rho_1 &= (t-t_{f1})^3(c_{10}+c_{11}(t-t_0)+c_{12}(t-t_0)^2)\\ T_1 &= \lambda_1(|\sigma_1(t_0)|^2+|\dot{\sigma}_1(t_0)|^3+|\ddot{\sigma}_1(t_0)|^6)^{1/6}.\end{aligned}$$

For the next state $\Sigma_2 = \sigma_2 - \rho_2,\ \sigma_2 = x_2 - \phi_1$ then

$$\begin{aligned}\phi_2(x_2,t,u_2) &= -0.7x_1x_2+u_2\\ \dot{u}_2 &= -\alpha_2 H_{1,2}(\Sigma_2,\dot{\Sigma}_2)\\ H_{1,2}(\Sigma_2,\dot{\Sigma}_2) &= \frac{\dot{\Sigma}_2+|\Sigma_2|^{1/2}\mathrm{sign}(\Sigma_2)}{|\dot{\Sigma}_2|+|\Sigma_2|^{1/2}}\\ \rho_2 &= (t-t_{f_2})^2(c_{20}+c_{21}(t-t_0))\\ T_2 &= \lambda_2(|\sigma_2(t_0)|+|\dot{\sigma}_2(t_0)|^2)^{1/2}.\end{aligned}$$

Finally for state x_3, $\Sigma_3 = \sigma_3 - \rho_3,\ \sigma_3 = x_3 - \phi_2$

$$\begin{aligned}u &= \frac{1}{2}\{1.5x_3^2+u_3\}\\ u_3 &= -\alpha_3\mathrm{sign}(\Sigma_3)\\ \rho_3 = (t-t_{f_3})(c_{30});\ T_3 &= \lambda_3(|\sigma_3(t_0)|).\end{aligned}$$

Results obtained in simulations are shown in figures (6.11)-(6.14), where the next parameters $\alpha_1 = 4,\ \alpha_2 = 10,\ \alpha_3 = 8,\ \lambda_1 = 6,\ \lambda_2 = 0.5,\ \lambda_3 = 1$ were used. In figures (6.11) and (6.12), the vector of initial conditions $x_\circ = [3,\ -2,\ 4]^T$ is used, whereas in figures (6.13) and (6.14), $x_\circ = [-3,\ 1.5,\ 2]^T$ was used and a phase lead of 30 seconds is introduced in y_d.

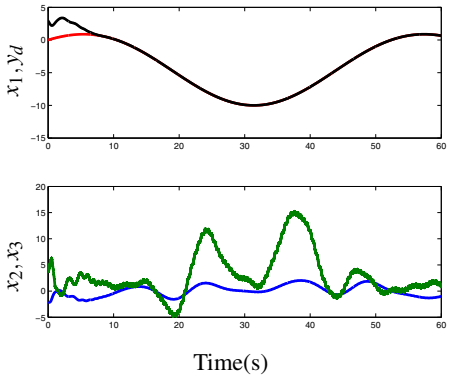

Fig. 6.11 States and reference evolution $(x(0) = [3, -2, 4]^T)$

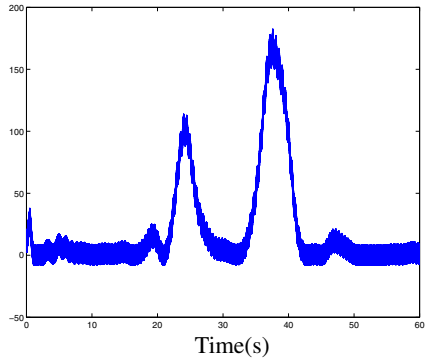

Fig. 6.12 Control signal u

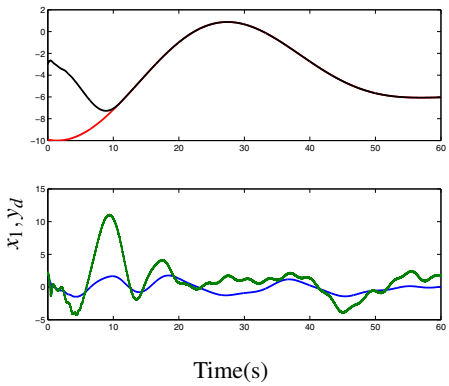

Fig. 6.13 States and reference evolution $(x(0) = [-3, 1.5, 2]^T)$

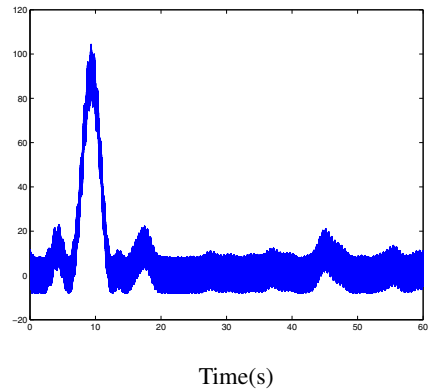

Fig. 6.14 Control signal u

6.2.4 *Exact Unmatched Uncertainties Compensation Based on HOSM Observation*

Let us consider a linear time invariant system with unknown inputs

$$\dot{x}(t) = Ax(t) + Bu(t) + D\omega(t),$$
$$y(t) = Cx(t),$$

where $x \in \mathbb{R}^n$, $u \in \mathbb{R}^m$, $y \in \mathbb{R}^p$ and $\omega \in \mathbb{R}^q$ are the state vector, the control, the measured output of the system and the unknown input (or disturbance), respectively. In addition, and without loss of generality, let us assume that $\operatorname{rank} C = p$, $\operatorname{rank} B = m$, $\operatorname{rank} D = q$ and that the triplet (A, D, C) is strongly observable, such that the

state $x(t)$ may be recovered in finite-time using only the output and its derivatives (through the use of the HOSM differentiator). Under the additional assumption on the smoothness of the unknown input w, i.e. $\|\dot{\omega}(t)\| \leq \omega^+$, an extra derivative of the estimated state can be computed, thus obtaining an estimate for $\dot{x}$. Under these considerations, an estimate for the unknown input may be obtained as

$$\hat{\omega} = D^+ \left[\dot{x}(t) - Ax(t) - Bu(t)\right],$$

With this estimate of the unknown input, it is natural to try to compensate the effect of the unknown input in the system as much as possible. Direct compensation of the part of $\omega(t)$ that is matched to u is possible. To see this apply the state transformation $\mathscr{T} = \begin{bmatrix} B^\perp \\ B^+ \end{bmatrix}$ which allows to rewrite the system as

$$\begin{aligned} \dot{x}_1(t) &= A_{11}x_1(t) + A_{12}x_2(t) + D_1\omega(t), \\ \dot{x}_2(t) &= A_{21}x_1(t) + A_{22}x_2(t) + D_2\omega(t) + u(t) \end{aligned} \tag{6.31}$$

with $x_1(t) \in \mathbb{R}^{n-m}$, $x_2(t) \in \mathbb{R}^m$. Then taking

$$u(t) = -D_2\hat{\omega}(t) + v(t),$$

the effect of matched disturbances can be reduced and, if all the derivatives are exact, completely removed without the direct application of a discontinuous control signal. Hence, $v(t) \in \mathbb{R}^m$, which may be designed following any control strategy, is a nominal control.

Another option is to consider the estimate of the disturbance into the sliding surface design in order to compensate the effects of the unmatched inputs. Thus, if

$$\operatorname{span} D_1 \in \operatorname{span} A_{12}, \tag{6.32}$$

the sliding surface is designed as $\sigma = x_2 + Kx_1 + G\hat{\omega}$, where matrices K and G are to be designed to provide for both stability and performance and the control is constructed as an unitary control

$$u(t) = -\varphi(x)\frac{\sigma}{\|\sigma\|}.$$

Now, to realize the reconstruction of the state, let us introduce a HOSM observer. The HOSM observer provides the theoretically exact value of the state vector and the unknown inputs identification in a finite time.

6.2.4.1 HOSM Observation and Identification Process

Basically, the HOSM observer design consists of two stages: firstly a Luenberger observer is used to maintain the norm of the estimation error bounded; then, by

means of a differentiation scheme, the state vector is reconstructed. For further details see [[4]].

Before introducing the observer, let us define the following notation: let $f(t)$ be a vector function, $f^{[i]}(t)$ represents the i-th anti-differentiator of $f(t)$, i.e. $f^{[i]}(t) = \int_0^t \int_0^{\tau_1} \cdots \int_0^{\tau_{i-1}} f(\tau_i)\, d\tau_i \cdots d\tau_2 d\tau_1$, $f^{[0]}(t) = f(t)$.

Stage 1. In order to realize the differentiation process we need to be sure that the observation error will be bounded. Firstly, design an auxiliary dynamic system

$$\dot{\tilde{x}}(t) = A\tilde{x}(t) + Bu(t) + L(y(t) - \tilde{y}, (t)),$$

where $\tilde{x} \in \mathbb{R}^n$ is an auxiliary state vector and $\tilde{y}(t) = C\tilde{x}(t)$ and the gain L must be designed such that the matrix $\tilde{A} := (A - LC)$ is Hurwitz (notice that strongly observable assumption implies that (A,C) pair is observable). Let $e(t) := x(t) - \tilde{x}(t)$, whose dynamic equations are

$$\dot{e}(t) = \tilde{A}e(t) + Dw(t). \tag{6.33}$$

Thus, in view of the boundness of the unknown input $\omega(t)$, $e(t)$ has a bounded norm, i.e., there exists a known constant e^+ and a finite time t_e, such that

$$\|e(t)\| \leq e^+, \text{ for all } t > t_e. \tag{6.34}$$

Stage 2. This part of the state reconstruction is based on an algorithm that allows decoupling the unknown inputs from the successive derivatives of the output of the linear estimation error system $y_e(t) := y(t) - C\tilde{x}(t)$.

0. Define $M_1 := C$.
1. Derive a linear combination of the output $y_e(t)$, ensuring that the derivative of this combination is unaffected by the uncertainties, i.e., $\frac{d}{dt}(M_1 D)^{\perp} y_e(t) = (M_1 D)^{\perp} C\tilde{A}e(t)$. Thus, form the extended vector

$$\begin{bmatrix} \frac{d}{dt}(M_1 D)^{\perp} y_e(t) \\ y_e(t) \end{bmatrix} = \underbrace{\begin{bmatrix} (M_1 D)^{\perp} C\tilde{A} \\ C \end{bmatrix}}_{M_2} e(t). \tag{6.35}$$

   Then, moving the differentiation operator outside the parenthesis and defining $J_1 = (M_1 D)^{\perp}$, the following equation is obtained

$$\frac{d}{dt} \begin{bmatrix} J_1 & 0 \\ 0 & I_p \end{bmatrix} \begin{bmatrix} y_e(t) \\ y_e^{[1]}(t) \end{bmatrix} = M_2 e(t), \tag{6.36}$$

   where $I_p \in \mathbb{R}^{p \times p}$ is an identity matrix.
2. Derive a linear combination of $M_2 e(t)$, ensuring that the derivative of this combination is unaffected by uncertainties, i.e. $\frac{d}{dt}(M_2 D)^{\perp} M_2 e(t)$. Then form the extended vector

$$\begin{bmatrix} \frac{d}{dt}(M_2D)^{\perp}M_2e(t) \\ y_e(t) \end{bmatrix} = \underbrace{\begin{bmatrix} (M_2D)^{\perp}C\tilde{A} \\ C \end{bmatrix}}_{M_3} e(t). \tag{6.37}$$

Moving the differentiation operator outside the parenthesis from (6.37) we have that

$$\frac{d}{dt}\begin{bmatrix} (M_2D)^{\perp}M_2e(t) \\ y_e^{[1]}(t) \end{bmatrix} = M_3e(t).$$

From the above expression and from (6.36), and by moving the differentiation operator outside the parenthesis, it yields to

$$\frac{d^2}{dt^2}\begin{bmatrix} J_2 & 0 \\ 0 & I_p \end{bmatrix}\begin{bmatrix} y_e(t) \\ y_e^{[1]}(t) \\ y_e^{[2]}(t) \end{bmatrix} = M_3e(t), \tag{6.38}$$

where $J_2 = (M_2D)^{\perp}\begin{bmatrix} J_1 & 0 \\ 0 & I_p \end{bmatrix}$.

j. A general step j ($j \geq 1$) can be summarized as follows. Derive $\left(M_{j-1}D\right)^{\perp}M_{j-1}e(t)$. Then, from the identity

$$\begin{bmatrix} \frac{d}{dt}\left(M_{j-1}D\right)^{\perp}M_{j-1}e(t) \\ y_e(t) \end{bmatrix} = \underbrace{\begin{bmatrix} \left(M_{j-1}D\right)^{\perp}M_{j-1}\tilde{A} \\ C \end{bmatrix}}_{M_j} e(t), \tag{6.39}$$

the next expression is obtained

$$\frac{d^{j-1}}{dt^{j-1}}\begin{bmatrix} J_{j-1} & 0 \\ 0 & I_p \end{bmatrix}\begin{bmatrix} y_e(t) \\ \vdots \\ y_e^{[j-1]}(t) \end{bmatrix} = M_je(t), \tag{6.40}$$

where $J_{j-1} = \left(M_{j-1}D\right)^{\perp}\begin{bmatrix} J_{j-2} & 0 \\ 0 & I_p \end{bmatrix}$.

Due to the strong observability assumption, there exists a unique positive integer k such that after k steps of the algorithm ($0 \leq k \leq n$), the matrix M_k generated recursively by (6.40), satisfies the conditions $\mathtt{rank}M_i < n$ for all $i < k$ and $\mathtt{rank}M_i = n$ for all $i \geq k$ (see, e.g., [[33]]). This means that the algebraic equation

$$M_ke(t) = \frac{d^{k-1}}{dt^{k-1}}\begin{bmatrix} J_{k-1} & 0 \\ 0 & I_p \end{bmatrix}\begin{bmatrix} y_e(t) \\ \vdots \\ y_e^{[k-1]}(t) \end{bmatrix}$$

has a unique solution for $e(t)$. Such solution may be found by pre-multiplying both sides of the previous equation by $M_k^+ := \left(M_k^T M_k\right)^{-1} M_k^T$. That is

$$e(t) = \frac{d^{k-1}}{dt^{k-1}} M_k^+ \begin{bmatrix} J_{k-1} & 0 \\ 0 & I_p \end{bmatrix} \begin{bmatrix} y_e(t) \\ \vdots \\ y_e^{[k-1]}(t) \end{bmatrix} \tag{6.41}$$

Thus, the term $e(t)$ can be reconstructed in just one step using a high order differentiation; meanwhile the matrices M_k and J_{k-1} should be obtained in an iterative manner using (6.39) with $M_1 = C$.

From (6.41), the reconstruction of $x(t)$ is equivalent to the reconstruction of $e(t)$, which can be carried out by a linear combination of the output $y_e(t)$ and its $(k-1)$-th derivatives. Hence, a real time high order sliding mode differentiator will be used in order to provide the theoretically exact observation and unknown inputs identification.

The bondness of $\dot{\omega}(t)$ allows realizing a $k-th$ order sliding mode differentiator, such that we recover not only the state $x(t)$ but also the disturbance $\omega(t)$. Beforehand, let us define

$$\Theta(t) := M_k^+ \begin{bmatrix} J_{k-1} & 0 \\ 0 & I_p \end{bmatrix} \begin{bmatrix} y_e(t) \\ \vdots \\ y_e^{[k-1]}(t) \end{bmatrix}. \tag{6.42}$$

That is, from (6.41) and (6.42)

$$e(t) = \frac{d^{k-1}}{dt^{k-1}} \Theta(t). \tag{6.43}$$

The HOSM differentiator is given by

$$\begin{aligned} \dot{z}_0(t) &= -\lambda_0 \Gamma^{\frac{1}{i+1}} \Psi^{\frac{i}{i+1}} (z_0(t) - \Theta(t)) + z_1(t) \\ \dot{z}_1(t) &= -\lambda_1 \Gamma^{\frac{1}{i}} \Psi^{\frac{i-1}{i}} (z_1(t) - \dot{z}_0(t)) + z_2(t) \\ &\vdots \\ \dot{z}_{k-1}(t) &= -\lambda_{k-1}(t) \Gamma^{\frac{1}{2}} \Psi^{\frac{1}{2}} (z_{k-1}(t) - \dot{z}_{k-2}(t)) + z_k(t) \\ \dot{z}_k(t) &= -\lambda_k \Gamma \Psi^0 (z_k(t) - \dot{z}_{k-1}(t)), \end{aligned} \tag{6.44}$$

where $z_i(t), \Theta(t) \in \mathbb{R}^n$, $\lambda_i, \Gamma \in \mathbb{R}$. Consider $\vartheta = \begin{bmatrix} \vartheta_1 & \dots & \vartheta_n \end{bmatrix}^T$, $\beta \in \mathbb{R}$, the function vector $\Psi^\beta(\sigma) \in \mathbb{R}^n$ is defined as $\Psi^\beta(\vartheta) = \begin{bmatrix} |\vartheta_1|^\beta sign(\vartheta_1) & \dots & |\vartheta_n|^\beta sign(\vartheta_n) \end{bmatrix}^T$.

In [[27]] there was shown that there is a finite time T such that the identity

$$z_j(t) = \frac{d^j}{dt^j} \Theta(t) \tag{6.45}$$

is achieved for every $j = 0, ..., k$.

The values of the λ's can be calculated as it is shown in [[27]], Γ is a Lipschitz constant of $\Theta^{(k+1)}(t)$, which for our case can be calculated in the following way: from (6.34) and (6.43) $\left\|\Theta^{(k-1)}(t)\right\| \leq e^{+}$, the next derivative $\Theta^{(k)}(t) = \dot{e}(t)$ will be also bounded $\left\|\Theta^{(k)}(t)\right\| \leq \left\|\tilde{A}\right\| e^{+} + \|B\|\,\omega^{+}$. Finally, it can be verified that

$$\Gamma \geq \left\|\tilde{A}\right\|^{2} e^{+} + \left\|\tilde{A}\right\| \|D\|\,\omega^{+} + \|D\|\,\omega^{+}. \tag{6.46}$$

The vector $e(t)$ can be reconstructed from the $(k-1)$-th order sliding dynamics. Thus from (6.45), we achieve the identity $z_{k-1}(t) = e(t)$, and consequently

$$\hat{x}(t) := z_{k-1}(t) + \tilde{x}(t) \text{ for all } t \geq T, \tag{6.47}$$

where $\hat{x}$ represents the estimated value of x. Therefore, the identity

$$\hat{x}(t) \equiv x(t) \tag{6.48}$$

is achieved, for all $t \geq T$.

Now, from error dynamics (6.33), we can recover $\dot{e}(t)$ using the HOSM differentiator (6.44). From (6.45), the equality $z_k(t) = \dot{e}(t)$ is achieved for all $t \geq T$ and the next equation holds

$$\hat{\omega}(t) = D^{+}\left[z_k(t) - \tilde{A} z_{k-1}(t)\right], \tag{6.49}$$

where $\hat{\omega}(t)$ is the identified exact value of the unknown input $\omega(t)$. Thus, after a finite time T, when the HOSM differentiator converges (see [[27]]), the identity $\hat{\omega}(t) \equiv \omega(t)$ holds.

6.2.4.2 Control Design

The sliding surface is designed considering the estimated values of the state and the identified unknown input signal, $\left[\hat{x}_1\ \hat{x}_2\right] \leftrightarrow \mathscr{T}\hat{x}$, as follows

$$s(t) = K\hat{x}_1(t) + \hat{x}_2(t) + G\hat{\omega}(t). \tag{6.50}$$

The matrix $K \in \mathbb{R}^{m\times(n-m)}$ could be designed to prescribe the required performance of the reduced-order system. The term $G\hat{w}(t)$ is added to compensate unmatched uncertainties. The control law given in (6.2.4) is considered. First, it is necessary guarantee that the above control law induces a sliding motion despite the presence of uncertainties.

Due to (6.48), the identities $\hat{x}_1 = x_1$, $\hat{x}_2 = x_2$ are certainly obtained. Then, the time derivative of $\sigma(t)$ is given by

$$\dot{\sigma}(t) = \Phi x(t) + (KD_1 + D_2)\,\omega(t) + G\dot{\hat{\omega}}(t) + u(t), \tag{6.51}$$

where matrix $\Phi \in \mathbb{R}^{m\times n}$ is defined as $\Phi := \left[KA_{11} + A_{21}\ KA_{12} + A_{22}\right]\mathscr{T}$.

Choosing a Lyapunov candidate function $V(\sigma) = \frac{\sigma^T(t)\sigma(t)}{2}$ and taking its derivative along time yields

$$\begin{aligned}\dot{V}(\sigma) &= \sigma^T(t)\left(\Phi x(t) + (KD_1 + D_2)\,\omega(t) + G\dot{\hat{\omega}}(t) - \varphi(x)\,\frac{\sigma(t)}{\|\sigma(t)\|}\right)\\ &\leq -\|\sigma(t)\|\,(\varphi(x) - \|\Phi\|\,\|x(t)\| - \theta)\end{aligned} \tag{6.52}$$

where $\theta := \|(KD_1 + D_2)\|\,\omega^+ + \|G\|\,\omega^+$. The scalar gain $\varphi(x)$ satisfies the condition

$$\varphi(x) - \|\Phi\|\,\|x(t)\| - \theta \geq \zeta > 0,$$

where ζ is a constant.

$$\varphi(x) > \|\Phi\|\,\|x(t)\| + \theta + \zeta. \tag{6.53}$$

Combining inequalities (6.52) and (6.53), it follows that the derivative of the Lyapunov function satisfies $\dot{V}(\sigma) \leq -\zeta V^{\frac{1}{2}}$ and, consequently, gain $\varphi(x)$ will induce the sliding motion.

When the system reaches the sliding surface $\sigma = 0$, we have

$$x_2(t) = -Kx_1(t) - G\hat{\omega}(t) \tag{6.54}$$

$$\dot{x}_1(t) = (A_{11} - A_{12}K)\,x_1(t) - A_{12}G\hat{\omega}(t) + D_1\omega(t). \tag{6.55}$$

It is well known that the (A_{11}, A_{12}) pair will be controllable since the (A, B) pair is controllable also [[12]]. Hence, there exists a matrix K such that matrix $A_s \triangleq (A_{11} - A_{12}K)$ has stable eigenvalues. The G gain matrix should be selected in order to compensate the unmatched uncertainties. In order to compensate $\omega(t)$ from $x_1(t)$, matrix D_1 must be matched with respect to A_{12}; therefore, im $(D_1) \subset$ im (A_{12}).

Thus, matrix $G \in \mathbb{R}^{m\times p}$ may be chosen so that

$$A_{12}G = D_1. \tag{6.56}$$

Then equation (6.55) yields

$$\dot{x}_1(t) = (A_{11} - A_{12}K)\,x_1(t) + D_1\,(\omega(t) - \hat{\omega}(t)), \tag{6.57}$$

so, in the ideal case after a finite time T, $w(t) \equiv \hat{\omega}(t)$, and therefore,

$$\dot{x}_1(t) = A_s x_1(t). \tag{6.58}$$

In particular, when $\mathtt{rank}(A_{12}) = n - m$, matrix $G = A_{12}^{+}D_1$.

Since the eigenvalues of A_s have negative real part, equation (6.58) is exponentially stable. Hence, the unmatched uncertainties are compensated and coordinate x_1

is stabilized. The trajectories of the state x_1 will converge to a bounded region, i.e. there exist some constants $a_1, a_2 > 0$ such that

$$\|x_1(t)\| \leq a_1 \|x_1(0)\| \exp^{-a_2 t} \quad \forall t > T_\sigma,$$

where T_σ is the time taken to reach the sliding surface. Furthermore, $x_2(t)$ is bounded as well indeed during sliding motion. Taking the norm of equation (6.54) we have

$$\|x_2(t)\| \leq \|K\| \|x_1(t)\| + \|G\| w^+ \quad \forall t > T_\sigma. \tag{6.59}$$

From the above equation, it is clear that the trajectories of $x_2(t)$ are bounded.

6.2.4.3 Simulations

Consider the inverted pendulum system shown in Fig. 6.15. The system consists of a cart (e) moving along a metal guiding bar (d). A cylindrical weight (f) is fixed to the cart by an axis (g). The cart is connected by a transmission belt (c) to a drive wheel (b). The wheel is driven by a current controlled direct current motor (a) which transforms the voltage u in torque such that the cart is accelerated. The state equations, considering the actuator dynamics are

$$\dot{x} = \begin{bmatrix} 0 & 0 & 1 & 0 & 0 \\ 0 & 0 & 0 & 1 & 0 \\ 0 & -\frac{m_p \ell^2 g}{(m_p+m_c)I+m_p m_c \ell^2} & 0 & 0 & \frac{K_t\left(I+m_p \ell^2\right)}{(m_p+m_c)I+m_p m_c \ell^2} \\ 0 & \frac{(m_p+m_c) m_p g \ell}{(m_p+m_c)I+m_p m_c \ell^2} & 0 & 0 & -\frac{m_p \ell K_t}{(m_p+m_c)I+m_p m_c \ell^2} \\ 0 & 0 & \frac{2\pi K_m}{I_m} & 0 & -\frac{R}{I_m} \end{bmatrix} x + \begin{bmatrix} 0 \\ 0 \\ 0 \\ 0 \\ \frac{1}{I_m} \end{bmatrix} u$$

$$+ \begin{bmatrix} 0 \\ 0 \\ \frac{I+m_p \ell^2}{(m_p+m_c)I+m_p m_c \ell^2} \\ -\frac{m_p \ell}{(m_p+m_c)I+m_p m_c \ell^2} \\ 0 \end{bmatrix} w \tag{6.60}$$

$$y = \begin{bmatrix} 1\,0\,0\,0\,0 \\ 0\,1\,0\,0\,0 \\ 0\,0\,0\,0\,1 \end{bmatrix} x, \tag{6.61}$$

The state vector is given by $x = \left[r \ \phi \ \dot{r} \ \dot{\phi} \ di/dt \right]^T$, where r, ϕ, i, represent the longitudinal position of the cart, the angular position of the pendulum and the motor current respectively. The unknown input ω is a perturbing force acting on the cart. The variable description and their corresponding values are given in the next table. For this example, we are considering an unknown input $\omega = 2.5 \sin(2.2t) + 1.5$.

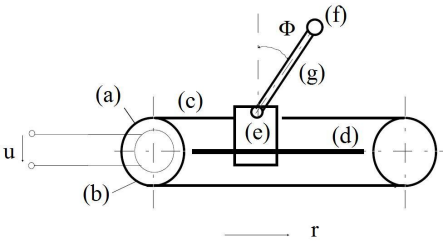

Fig. 6.15 Inverted cart pendulum system

Table 6.1 Inverted-Cart Pendulum System description

Symbol	Description	Value	Units
m_p	mass of the pendulum	0.36	kg
m_c	mass of the cart	4	kg
I	pendulum moment of inertia	0.084	$kg \cdot m^2$
ℓ	longitude	0.5	m
g	gravitational acceleration constant	9.81	m/s^2
K_t	motor torque constant	0.0295	$N \cdot m$
I_m	motor inductance	0.0087	H
K_m	motor back electromotive constant	0.212	$V/(rad/s)$
R	motor armature resistance	3.12	Ω

Observer design. First, a Luenberger-type observer is designed such that matrix $A - LC$ has a set of eigenvalues given by $\{-780, -9, -2.6, -2\}$. System (6.62)-(6.63) is strongly observable. A way to check the system's strong observability property is to apply the unknown inputs decoupling algorithm introduced in Observer Section. Thus, if the system is strongly observable, k iterations $(k \leq n)$ are needed to find a full column rank matrix M_k. For system (6.62)-(6.63) $k = 2$. From (6.41) we need to differentiate once $(i.e.\ (k-1) - times)$ in order to reconstruct the state. Additionally, for recovering the unknown inputs a second differentiation is needed. The total order of the differentiator (6.44) is determined by the smoothness of the unknown input, we select a HOSM differentiator of $2^{nd} - order$. The input of the HOSM differentiator (6.42) is

$$\Theta(t) = \begin{bmatrix} -0.07 & 0 & 0 & 0.45 & 0.05 & 0.48 \\ 0 & 0 & 0 & 0.05 & 0.99 & -0.48 \\ -0.32 & 0 & 0 & -2.4 & 0.18 & -2.76 \\ 0.76 & 1 & 0 & 4.22 & 9.16 & 3.83 \\ 0.06 & 0 & 0 & 0.48 & -0.04 & 0.56 \end{bmatrix} \begin{bmatrix} y_e(t) \\ y_e^{[1]}(t) \end{bmatrix}.$$

Following [[27]] we select $\lambda_0 = 1.1, \lambda_1 = 1.5, \lambda_2 = 2$.The observer gain is $\Gamma = 2.8e6$. The sampling step is $\delta = 10(\mu s)$.

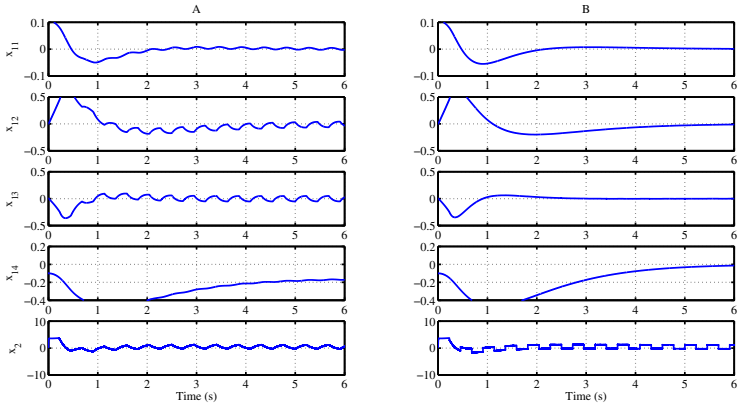

Fig. 6.16 Column (B) shows the compensated system and in column (A) the system without compensation. The underactuated states are $x_{11},\ldots,x_{14}$, while the completely actuated state is x_2

Control design. Regularizing the system

$$\dot{x}_1 = \begin{bmatrix} 0 & 0 & 1 & 0 \\ -0.4377 & 0 & 0 & 0 \\ 10.6 & 10 & 0 & 0 \\ 0 & -1 & 0 & 0 \end{bmatrix} x_1 + \underbrace{\begin{bmatrix} 0 \\ 0.8345 \\ -0.8632 \\ 0 \end{bmatrix}}_{A_{12}} x_2 + \underbrace{\begin{bmatrix} 0 \\ 0.2396 \\ -0.2479 \\ 0 \end{bmatrix}}_{D_1} \omega \tag{6.62}$$

$$\dot{x}_2 = \begin{bmatrix} 0 & -1.332 & 0 & 0 \end{bmatrix} x_1 - 386.35u. \tag{6.63}$$

From the above equation can be seen that condition im $(D_1) \subset \text{im}(A_{12})$ is satisfied. The compensator gain is selected as $G = 0.28$. The gain K was designed by eigenvalues assignment, such that the reduced order system has an eigenvalues set given by $\{-1-1.3-4.53-3.9\}$. From (6.53) the sliding mode gain is selected as $\varphi(x) = 1.2e3\,(\|x(t)\|+1)$.

The simulation was carried comparing two approaches for sliding surface design. The approach in (A) was carried designing a conventional sliding mode surface (see [[37]]) i.e. $\sigma_A(t) = x_1(t) + Kx_2(t)$, while in (B), the surface was designed to cope with the unmatched perturbations (6.50) i.e. $\sigma_B(t) = x_1(t) + Kx_2(t) + G\hat{\omega}(t)$. Fig. (6.16) shows the states of the regularized system, column (A) shows the results when no compensation is carried: the perturbation effects are present in all the states. Column (B) shows the states when the compensation of unmatched uncertainties is done through the sliding surface, here the stabilization of state x_1 is achieved, while the trajectories of state x_2 remain bounded.

6.2.5 Conclusions

Three methods for finite time compensation of unmatched perturbations of inputs are suggested.

Open problems:

1. Design a global compensation technique joining the Lyapunov backstepping techniques together with HOSM techniques.

2. Observer based compensation for the case when condition (6.32) is not satisfied.

References

1. Adhami-Mirhosseini, A., Yazdanpanah, M.J.: Robust Tracking of perturbed systems by nested sliding mode control. In: Proc. of the International conference on Control and Automation, Budapest, Hungary, pp. 44–48 (2005)
2. Angulo, M., Fridman, L., Levant, A.: Exact Finite-Time Output Based Control using High-Order Sliding Modes. International Journal of Systems Science 42(11), 1847–1857 (2011)
3. Bartolini, G., Ferrara, A., Giacomini, L., Usai, E.: A combined backstepping/second order sliding mode approach to control a class of non-linear systems. In: Proceedings of the IEEE International Workshop on Variable Structure Systems, Tokyo, Japan, pp. 205–210 (1996)
4. Bejarano, F.J., Fridman, L.: High order sliding mode observer for linear systems with unbounded unknown inputs. International Journal of Control 83(9), 1920–1929 (2010)
5. Cao, W., Xu, J.: Nonlinear integral-type sliding surface for both matched and unmatched uncertain systems. IEEE Trans. Automat. Contr. 49, 1355–1360 (2004)
6. Castaños, F., Fridman, L.: Analysis and Design of Integral Sliding manifolds for Systems With Unmatched Perturbations. IEEE Trans. Automat. Contr. 51(5), 853–858 (2006)
7. Choi, H.H.: An LMI-based switching surface design method for a class of mismatched uncertain systems. IEEE Trans. Automat. Contr. 48, 1634–1638 (2003)
8. Choi, H.H.: Output feedback variable structure control design with an H_2 performance bound constraint. Automatica 48(9), 2403–2408 (2008)
9. Davis, R., Spurgeon, S.K.: A nonlinear control strategy for robust sliding mode performance in the presence of unmatched uncertainty. International Journal of Control 57, 1107–1123 (1993)
10. Davis, R., Spurgeon, S.K.: Robust implementation of sliding mode control schemes. International Journal of System Science 24, 733–743 (1993)
11. Drazenovic, B.: The Invariance Conditions in Variable Structure Systems. Automatica 5(3), 287–295
12. Edwards, C., Spurgeon, S.K.: Sliding Mode Control. Taylor and Francis, London (1998)
13. Yan, X.G., Spurgeon, S.K., Edwards, C.: Dynamic sliding mode control for a class of systems with mismatched uncertainty. European Journal of Control 11(1), 1–10 (2005)

14. Estrada, A., Fridman, L.: Integral HOSM Semiglobal Controller for Finite-Time Exact Compensation of Unmatched Perturbations. IEEE Trans. Automat. Contr. 55(11), 2644–2649 (2010)
15. Estrada, A., Fridman, L.: Quasi-continuous HOSM control for systems with unmatched perturbations. Automatica 46(11), 1916–1919 (2010)
16. Ferrara, A., Giacomini, L.: On multi-input backstepping design with second order sliding modes for a class of uncertain nonlinear systems. International Journal of Control 71(5), 767–788 (1998)
17. Ferreira de Loza, A., Bejarano, F.J., Fridman, L.: Unmatched uncertainties compensation based on high-order sliding mode observation. International Journal on Robust and Nonlinear Control (2012), doi:10.1002/rnc.2795
18. Filippov, A.F.: Differential Equations with Discontinuous Right-Hand Side. Kluwer, Dordrecht (1988)
19. Fridman, L.: Singularly perturbed analysis of chattering in relay control systems. IEEE Transactions on Automatic Control 47(12), 2079–2084 (2079)
20. Huerta-Avila, H., Loukianov, A.G., Cañedo, J.M.: Nested Integral Sliding Modes of Large Sacale Power Systems. In: Proc. of the 46th IEEE Conference on Decision and Control, New Orleans, LA, USA, pp. 1993–1998 (December 2007)
21. Freeman, R.A., Kokotovic, P.V.: Robust Nonlinear Control Design. Birkhauser, Boston (1996)
22. Isidori, A.: Nonlinear Control Systems, 2nd edn. Springer, New York (1989)
23. Kanellakopoulos, I., Kokotović, P.V., Morse, A.S.: Systematic design of adaptive controllers for feedback linearizable system. IEEE Trans. on Automatic Control 36(11), 1241–1253 (1991)
24. Krstic, M., Kanellakopoulous, I., Kokotovic, P.: Nonlinear and Adaptive Control Design. Wiley Interscience, NY (1995)
25. Levant, A., Alelishvili, L.: Integral High-Order Sliding Modes. IEEE Trans. Automat. Contr. 52(7), 1278–1282 (2007)
26. Levant, A.: Quasi-Continuous High-Order Sliding-Mode Controllers. IEEE Trans. Automat. Contr. 50(11), 1812–18162 (2005)
27. Levant, A.: High-order sliding modes: differentiation and output-feedback control. International Journal of Control 76, 924–941 (2003)
28. Levant, A., Michael, A.: Adjustment of high-order sliding-mode controllers. International Journal of Robust and Nonlinear Control 19(15), 1657–1672 (2009)
29. Loukyanov, A., Utkin, V.: Methods of reducing equations for dynamic systems to a regular form. Automatic and Remote Control 42(4), 413–420 (1993)
30. Loukianov, A.G.: Nonlinear Block Control with Sliding Mode. Automation and Remote Control 59(7), 916–933 (1998)
31. Loukianov, A.G.: Robust Block Decomposition Sliding Mode Control Design. Mathematical Problems in Engineering 8(4-5), 349–365 (2002)
32. Loukianov, A., Caedo, J., Fridman, L., Soto Cota, A.: High order block sliding mode controller for a synchronous generator with an exciter system. IEEE Transactions on Industrial Electronics 58(1), 337–347 (2011)
33. Molinari, B.P.: A strong controllability and observability in linear multivariable control. IEEE Transactions on Automatic Control 21(5), 761–764 (1976)
34. Scarratt, J.C., Zinober, A.S.I., Mills, R.E., Rios-Bolivar, M., Ferrara, A., Giacomini, L.: Dynamical adaptive first and second-order sliding backstepping control of nonlinear nontriangular uncertain systems. ASME Journal of Dynamic Systems, Measurement and Control 122(4), 746–752 (2000)

35. Shtessel, Y.B., Buffington, J., Banda, S.: Multiple Time Scale Flight Control Using Reconfigurable Sliding Modes. In: Proceedings of the 37th IEEE Conference on Decision and Control, Tampa, Florida, USA, pp. 4196–4201 (December 1998)
36. Won, M.C., Hedrick, J.K.: Multiple surface sliding control of a class of uncertain nonlinear systems. International Journal of Control 64(4), 693–706 (1996)
37. Utkin, V.I.: Sliding modes in control and optimization. Springer, Berlin (1992)
38. Utkin, V.I., Guldner, J., Shi, J.: Sliding Mode Control in Electromechanical Systems. Taylor & Francis, London (1999)